



EFFECTS OF THERMAL RADIATION AND CHEMICAL REACTION ON AN UNSTEADY FORCED AND FREE CONVECTION FLOW PAST AN INFINITE PERMEABLE VERTICAL PLATE



S. Usman^{1*}, I. Abdullahi¹, B. G. Agaie¹ and H. B. Yusuf²

¹Department of Mathematics, Federal University Dutse (FUD), PMB 7156, Jigawa State, Nigeria

²Department of Mathematics, Nigerian Army University Biu, PMB 1500, Borno State, Nigeria

*Corresponding author: princemagee1@gmail.com, usman.sani@fud.edu.ng

Received: August 13, 2020 Accepted: November 09, 2020

Abstract: One dimensional free and forced convection flow of a viscous incompressible fluid through an infinite permeable vertical plate controlled by suction/injection(S_*) was studied. Temperature(θ), velocity(u), concentration(C) and skin friction(τ) profiles for the fluid were obtained and solved using He-Laplace method, where the thermal radiation and chemical reaction effects on the flow of the fluid together with the influence of each physical parameters were discussed with the aid of graphs. Observations were seen that the temperature(θ), velocity(u) and concentration(C) reduces with increasing suction/injection(S_*) near the plate boundary while the velocity(u) increases with increase in Grashof number(Gr). Also it was observed that the skin friction(τ) decreases with increasing suction/injection(S_*).

Keywords: Suction/injection, free & forced convection, permeable vertical plate, unsteady flow

Introduction

Forced and free convective flow through different channels is of considerable interest in many industrial applications such as drying process, geophysics among others. Fluctuating thermal and mass diffusion on unsteady free convection flow past a vertical plate in slip-flow regime was investigated by Sharma (2005), where it was seen that velocity tend to increase with increase in both Grashof and modified Grashof number. The mean skin friction increases with increase either the Grashof number or the modified Grashof number, but it decreases with increase in the rare fraction parameter. Unsteady MHD free convective flow past a vertical porous plate immersed in a porous medium with Hall current, thermal diffusion and heat source was studied by Ahmed *et al.* (2010) and it was found that the concentration at the plate surface increases under Soret effect which intend causes the main flow shear stress to rise and the cross flow shear stress to fall. Narahari and Nayan (2011) analytically studied free convection flow near an impulsively started infinite vertical plate with Newtonian heating in the presence of thermal radiation and constant mass diffusion. It was observed that the velocity decreases with increasing Schmidt number and radiation parameter and also the skin friction decreases in the presence of aiding flows whereas it increases in the presence of opposing flows. Shivaiah and Rao (2012) analyzed the effect of chemical reaction on unsteady magneto hydrodynamic free convective fluid flow past a vertical porous plate in the presence of suction or injection. Daniel *et al.* (2013) investigated an unsteady forced and free convection flow past an infinite permeable vertical plate and observed that temperature is higher near the plate with injection and velocity is more enhanced near the plate with both suction and injection. Unsteady MHD free convective heat and mass transfer flow past a semi-infinite vertical permeable moving plate with heat absorption, radiation, chemical reaction Soret effects was investigated by Rao *et al.* (2013) and observed that the presence of Soret effect brought about the reduction in the concentration distribution will lead to decrease in the fluid velocity. Vedavathi *et al.* (2014) looked at the radiation and mass transfer effects on unsteady MHD convective flow past an infinite vertical plate with Dufour and Soret effects and it was found that there was increase in the rate of mass transfer as a result of increase in the Schmidt number.

Javaherdeh *et al.* (2015) investigated two dimensional steady laminar free convection flow with heat and mass transfer past on a moving vertical plate in a porous medium subjected to a

transverse magnetic field and it was observed that a type of resistive force was produced which intend opposes the flow due to the presence of the transverse magnetic field. Malapati and Polarapu (2015) studied unsteady MHD free convective heat and mass transfer in a boundary layer flow past a vertical permeable plate with thermal radiation and chemical reaction where an increase in the rare fraction parameter causes an increase in the velocity of the fluid flow. Effect of thermal conductivity on magneto hydrodynamic heat and mass transfer in porous medium saturated with Kuvshinshiki fluid was studied by Idowu and Jimoh (2017) where, as radiation and thermal conductivity increases the velocity and temperature profile increases also. Babu and Reddy (2017) investigated the effect of thermal and chemical reaction on unsteady MHD free convection past a linear accelerated vertical porous plate with variable temperature and mass diffusion and it was observed that both velocity and concentration decreases with an increase in the Schmidt number. Thermal radiation and MHD effects on the unsteady free convection and mass transform flow past an exponentially accelerated vertical plate with variable temperature a finite element solution was also studied by Srilatha and Shekar (2018) and the skin friction was seen to increase with expansion in the Schmidt number intend cooling the plate and also a reverse case was found for heating of the plate. Arifuzzaman *et al.* (2018) investigated the chemically reactive and naturally convective high speed MHD fluid flow through an oscillatory vertical porous plate with heat and radiation absorption effect and it was observed that velocity profile and skin friction decreases due to increase in the magnetic parameter.

Based on the related literatures presented above, it is seen that the effects of heat and mass on an unsteady forced and free convection flow past an infinite permeable vertical plate have not been considered which is of importance to this field and hence the aim of this study and also to see the effect of heat and mass on the flow of the fluid as one of the objectives.

Mathematical Formulation

A natural unsteady forced and free convection flow of a viscous incompressible fluid with thermal and chemical effects past an infinite heated vertical permeable plate is considered with suction and injection. Taking the permeable plate to be in a vertical position parallel to the x' -axis and the

y' -axis taken normal to the plate. Also the physical variables are functions of y' and t' only.

Considering a two dimensional flow so that $\vec{V} = (u, v, 0)$, where u and v are the vertical and horizontal components of velocity respectively. But the flow is along the x' -axis which is a full flow and is a function of y' only. The governing equation of the flow are given as,

Equation of Continuity:

$$\frac{\partial u}{\partial y} = 0. \tag{1}$$

Integrating Eq. (1) we have the horizontal velocity as $u = v_0$ (a constant) which is the velocity of suction/injection.

Using the usual Boussinesq's approximation, we have,

Equation of Motion:

$$\rho \frac{\partial u'}{\partial t'} - v_0 \rho \frac{\partial u'}{\partial y'} = g\beta\rho(T' - T_\infty) + \rho g\beta^*(C' - C_\infty) + \mu \frac{\partial^2 u'}{\partial y'^2}. \tag{2}$$

Equation of Energy:

$$\rho C_p \frac{\partial \theta'}{\partial t'} - v_0 \frac{\partial \theta'}{\partial y'} = k \frac{\partial^2 \theta'}{\partial y'^2} - \frac{\partial q_r}{\partial y'} + \frac{Q_c}{\rho C_p} (C' - C_\infty). \tag{3}$$

Equation of Concentration:

$$\frac{\partial C'}{\partial t'} - v_0 \frac{\partial C'}{\partial y'} = D \frac{\partial^2 C'}{\partial y'^2} - KrC'. \tag{4}$$

Here, u' is the component of velocity in the direction of y' -axis, t' is the time, g is the acceleration due to gravity, β and β^* are the coefficient of volume expansion for heat and mass transfer, θ' and C' are the fluid temperature and concentration, ρ is the density of the fluid, μ the coefficient of viscosity, θ_∞ is the temperature far from the plate, C_∞ molar concentration far from the plate, C_p is the specific heat, k thermal conductivity, Q_c is the constant heat flux per unit area, D is the diffusion coefficient of the diffusing species, Kr is the chemical reaction parameter and q_r is the radiation heat flux according to Rosseland approximation where

$$q_r = -\frac{16\sigma^* \theta^3}{3k^*} \frac{\partial \theta}{\partial y}. \tag{5}$$

Given that σ^* is the Stefan-Boltzman constant, k^* is the mean absorption coefficient, θ_w' and C_w' are the temperature and molar concentration near the plate.

The initial and boundary conditions are,

$$u'(y, t) = u_0 e^{-y}, \theta'(y, t) = (\theta_w' - \theta_\infty) e^{-y} + \theta_\infty, \theta'(y, t) = (C_w' - C_\infty) e^{-y} + C_\infty,$$

$t' \leq 0$, for all y' , and

$$u'(y, t) = 1, \theta'(y, t) = 1, C'(y, t) = 1, t' > 0, y' = 0. \tag{6}$$

On introducing the following non-dimensional quantities

$$y = \frac{y' u_0 Gr^{\frac{1}{2}}}{v}, t = \frac{t' u_0^2 Gr}{v^2}, u = \frac{u'}{u_0}, \theta = \frac{\theta' - \theta_\infty}{\theta_w' - \theta_\infty}, C = \frac{C' - C_\infty}{C_w' - C_\infty}. \tag{7}$$

Substituting Eq. (7) in Eq. (2), (3) and (4) and applying the boundary condition (6) to obtain

$$\frac{\partial u}{\partial t} = S_* \frac{\partial u}{\partial y} + Gr\theta + GmC + \varphi \frac{\partial^2 u}{\partial y^2}. \tag{8}$$

$$\frac{\partial \theta}{\partial t} - S_* \frac{\partial \theta}{\partial y} = \frac{1}{Pr} \frac{\partial^2 \theta}{\partial y^2} + REc \frac{\partial^2 \theta}{\partial y^2} + \alpha_c C. \tag{9}$$

$$\frac{\partial C}{\partial t} - S_* \frac{\partial C}{\partial y} = \frac{1}{Sc} \frac{\partial^2 C}{\partial y^2} - Kr_* C + Nc. \tag{10}$$

Subject to the following initial and boundary conditions

$$t \leq 0, u(y, 0) = e^{-y}, \theta(y, 0) = e^{-y}, C(y, 0) = e^{-y},$$

for all y ,

$$t > 0, u(0, t) = 1, \theta(0, t) = 1, C(0, t) = 1, \text{ as } y = 0, \tag{11}$$

Where: the parameters below encompass the physics of the problem;

$$S_* = \frac{v_0}{u_0 Gr^{\frac{1}{2}}} \text{ (suction/injection parameter),}$$

$$Gm = \frac{v g \beta^* (C_w' - C_\infty)}{u_0^3 Gr} \text{ (Modified solutal Grashof number),}$$

$$Gr = \frac{v g \beta (\theta_w' - \theta_\infty)}{u_0^3 Gr} \text{ (Modified thermal Grashof number),}$$

$$\varphi = \frac{\mu}{v \rho} \text{ (constant term),}$$

$$Nc = \frac{v Kr C_\infty'}{u_0^2 Gr (C_w' - C_\infty')} \text{ (concentration difference parameter),}$$

$$Kr_* = \frac{v Kr}{u_0^2 Gr} \text{ (chemical reaction parameter),}$$

$$Sc = \frac{v}{D} \text{ (Schmidt number),}$$

$$Pr = \frac{v \rho C_p}{k} \text{ (Prandtl number),}$$

$$R = \frac{16 \sigma^* v \theta^3}{3 k^* u_0^4 Gr} \text{ (Radiation parameter),}$$

$$Ec = \frac{u_0^2}{C_p (\theta_w' - \theta_\infty')} \text{ (Eckert number),}$$

$$\alpha_c = \frac{v Q_c (C_w' - C_\infty')}{\rho^2 C_p^2 Gr u_0^2 (\theta_w' - \theta_\infty')} \text{ (Radiation absorption parameter).}$$

Method of Solution

Employing the method of solution known as He-Laplace method by Hradayesh and Atulya (2012), where the use of the Homotopy perturbation method coupled with Laplace transform method to solve linear and nonlinear partial differential equations. To illustrate the basic idea of this method, let us consider a general nonlinear nonhomogeneous partial differential equation with initial conditions of the form

$$\frac{\partial^2 y}{\partial t^2} + R_1 y(x, t) + R_2 y(x, t) + N y(x, t) = f(x, t)$$

$$y(x, 0) = \alpha(x), \frac{\partial y}{\partial t}(x, 0) = \beta(x), \tag{12}$$

Where: $R_1 = \frac{\partial^2}{\partial x^2}$ and $R_2 = \frac{\partial}{\partial x}$ are the linear differential operators, N represents the general nonlinear differential operator and $f(x, t)$ is the source term. Taking the Laplace transform (denoted by \mathcal{L}) on both side of Eq.(12), we have

$$\mathcal{L} \left\{ \frac{\partial^2 y}{\partial t^2} \right\} + \mathcal{L} \{R_1 y(x, t) + R_2 y(x, t)\} + \mathcal{L} \{N y(x, t)\} = \mathcal{L} \{f(x, t)\}$$

$$S^2 \mathcal{L} \{y(x, s)\} - S y(x, 0) - \frac{\partial y}{\partial t}(x, 0) = -\mathcal{L} \{R_1 y(x, t) + R_2 y(x, t)\} - \mathcal{L} \{N y(x, t)\} + \mathcal{L} \{f(x, t)\}. \tag{13}$$

Applying the initial conditions given in Eq.(12), we have

$$\mathcal{L} \{y(x, s)\} = \frac{\alpha(x)}{s} + \frac{\beta(x)}{s^2} - \frac{1}{s^2} \{ \mathcal{L} \{R_1 y(x, t) + R_2 y(x, t)\} + \mathcal{L} \{N y(x, t)\} \} + \frac{1}{s^2} \{ \mathcal{L} \{f(x, t)\} \}. \tag{14}$$

Operating the inverse Laplace transform on both sides of Eq.(14) gives

$$y(x, t) = F(x, t) - \mathcal{L}^{-1} \left\{ \frac{1}{s^2} \{ \mathcal{L} \{R_1 y(x, t) + R_2 y(x, t)\} + \mathcal{L} \{N y(x, t)\} \} \right\}, \tag{15}$$

where $F(x, t)$ represents the terms arising from the source term and the prescribed initial conditions. Now we apply the Homotopy perturbation method

$$y(x, t) = \sum_{n=0}^{\infty} P^n y_n(x, t), \tag{16}$$

and the nonlinear term can be decomposed as

$$N y(x, t) = \sum_{n=0}^{\infty} P^n H_n(y) \tag{17}$$

and

$$H_n(y) = \frac{1}{n!} \frac{\partial^n}{\partial P^n} N \left[\sum_{k=0}^n P^k y_k \right]_{P=0}. \tag{18}$$

Coupling the Laplace transform and the Homotopy perturbation method gives

$$\sum_{n=0}^{\infty} P^n y_n(x, t) = F(x, t) - P \left\{ \mathcal{L}^{-1} \left\{ \frac{1}{s^2} \{ \mathcal{L} \{R_1 + R_2\} \sum_{n=0}^{\infty} P^n y_n(x, t) + \sum_{n=0}^{\infty} P^n H_n(y) \} \right\} \right\} \tag{19}$$

So comparing the coefficients of like powers of P , we have the following approximations

$$\begin{aligned} P^0: y_0(x, t) &= F(x, t), \\ P^1: y_1(x, t) &= -\mathcal{L}^{-1} \left\{ \frac{1}{s^2} \mathcal{L} \{ (R_1 + R_2) y_0(x, t) + H_0(y) \} \right\}, \\ P^2: y_2(x, t) &= -\mathcal{L}^{-1} \left\{ \frac{1}{s^2} \mathcal{L} \{ (R_1 + R_2) y_1(x, t) + H_1(y) \} \right\}, \\ P^3: y_3(x, t) &= -\mathcal{L}^{-1} \left\{ \frac{1}{s^2} \mathcal{L} \{ (R_1 + R_2) y_2(x, t) + H_2(y) \} \right\}, \\ &\vdots \\ &\vdots \end{aligned} \tag{20}$$

Hence, the general solution takes the form

$$y(x, t) = y_0(x, t) + y_1(x, t) + y_2(x, t) + y_3(x, t) + \dots \tag{21}$$

Results and Discussion

Solving Eq.(8),(9) and (10) subject to the initial condition in Eq.(11) by the above discussed method, we obtain the following results

$$C(y, t) = e^{-y} + tNc - S_*e^{-yt} + \frac{e^{-yt}}{Sc} - Kr_*e^{-yt} - \frac{Kr_*Nct^2}{2!} + \frac{S_*^2e^{-yt^2}}{2!} - \frac{S_*e^{-yt^2}}{Sc2!} + \frac{S_*Kr_*e^{-yt^2}}{2!} - \frac{S_*e^{-yt^2}}{Sc2!} + \frac{e^{-yt^2}}{Sc^22!} - \frac{Kr_*e^{-yt^2}}{Sc2!} + \frac{S_*Kr_*e^{-yt^2}}{2!} - \frac{Kr_*e^{-yt^2}}{2!} + \frac{Kr_*^2e^{-yt^2}}{2!} + \frac{Kr_*^2Nct^3}{3!} - \frac{S_*^3e^{-yt^3}}{3!} + \frac{S_*^2e^{-yt^3}}{Sc3!} - \frac{S_*^2Kr_*e^{-yt^3}}{3!} + \frac{S_*^2e^{-yt^3}}{Sc3!} + \frac{S_*e^{-yt^3}}{Sc^23!} + \frac{S_*Kr_*e^{-yt^3}}{Sc3!} - \frac{S_*^2Kr_*e^{-yt^3}}{3!} + \frac{S_*Kr_*e^{-yt^3}}{3!} - \dots \quad (22)$$

$$\theta(y, t) = e^{-y} + \alpha_c e^{-yt} + \frac{\alpha_c Nct^2}{2!} - \frac{\alpha_c S_* e^{-yt^2}}{2!} + \frac{\alpha_c e^{-yt^2}}{Sc2!} - \frac{\alpha_c Kr_* e^{-yt^2}}{2!} - \frac{\alpha_c Kr_* Nct^3}{3!} + \frac{\alpha_c S_*^2 e^{-yt^3}}{3!} - \frac{\alpha_c S_* e^{-yt^3}}{Sc3!} + \frac{\alpha_c S_* Kr_* e^{-yt^3}}{3!} - \frac{\alpha_c S_* e^{-yt^3}}{Sc3!} + \frac{\alpha_c S_*^2 e^{-yt^3}}{Sc^23!} - \frac{\alpha_c S_*^2 Kr_* e^{-yt^3}}{3!} + \frac{\alpha_c S_*^2 e^{-yt^3}}{Sc^23!} + \frac{\alpha_c S_*^2 Kr_* e^{-yt^3}}{3!} + \frac{\alpha_c S_*^2 e^{-yt^3}}{Sc^23!} + \frac{\alpha_c S_*^2 Kr_* e^{-yt^3}}{3!} + \frac{\alpha_c S_*^2 e^{-yt^3}}{Sc^23!} + \frac{\alpha_c S_*^2 Kr_* e^{-yt^3}}{3!} + \frac{\alpha_c S_*^2 e^{-yt^3}}{Sc^23!} + \frac{\alpha_c S_*^2 Kr_* e^{-yt^3}}{3!} + \dots \quad (23)$$

$$u(x, t) = e^{-y} + Gre^{-yt} + \frac{\alpha_c Gre^{-yt^2}}{2!} + \frac{\alpha_c GrNct^3}{3!} - \frac{\alpha_c S_* Gre^{-yt^3}}{3!} + \frac{\alpha_c Gre^{-yt^3}}{Sc3!} - \frac{\alpha_c Kr_* Gre^{-yt^3}}{3!} - \frac{\alpha_c Kr_* GrNct^4}{4!} + \frac{\alpha_c S_*^2 Gre^{-yt^4}}{4!} - \frac{\alpha_c S_* Gre^{-yt^4}}{Sc4!} + \frac{\alpha_c S_* Kr_* Gre^{-yt^4}}{4!} - \frac{\alpha_c S_* Gre^{-yt^4}}{Sc4!} + \frac{\alpha_c Gre^{-yt^4}}{Sc^24!} - \frac{\alpha_c Kr_* Gre^{-yt^4}}{Sc4!} + \frac{\alpha_c S_* Kr_* Gre^{-yt^4}}{4!} - \frac{\alpha_c Kr_* Gre^{-yt^4}}{4!} + \frac{\alpha_c Kr_*^2 Gre^{-yt^4}}{4!} + \frac{\alpha_c Kr_*^2 GrNct^5}{5!} - \frac{\alpha_c S_*^3 Gre^{-yt^5}}{5!} + \frac{\alpha_c S_*^2 Gre^{-yt^5}}{Sc5!} - \frac{\alpha_c S_*^2 Kr_* Gre^{-yt^5}}{5!} + \frac{\alpha_c S_*^2 Gre^{-yt^5}}{Sc5!} - \frac{\alpha_c S_* Gre^{-yt^5}}{Sc^25!} + \frac{\alpha_c S_* Kr_* Gre^{-yt^5}}{Sc5!} - \frac{\alpha_c S_*^2 Kr_* Gre^{-yt^5}}{5!} + \frac{\alpha_c S_* Kr_* Gre^{-yt^5}}{5!} - \frac{\alpha_c S_*^2 Gre^{-yt^5}}{Sc5!} - \frac{\alpha_c S_* Gre^{-yt^5}}{Sc^25!} + \frac{\alpha_c Gre^{-yt^5}}{Sc^35!} - \dots \quad (24)$$

Now studying the skin friction given by

$$\tau' = -\mu \frac{\partial u}{\partial y}, \text{ at } y = 0. \quad (25)$$

In view of Eq. (7), Eq. (25) reduces to

$$\tau = \frac{-\tau'}{\rho u_0^2 Gr^{\frac{1}{2}}} = \frac{\partial u}{\partial y} \text{ at } y = 0. \quad (26)$$

Finding $\frac{\partial u}{\partial y}$ at $y = 0$ from Eq. (24) and substituting the solution into Eq. (26) and simplifying, we obtain the required skin friction.

Three basic equations that governed the flow through an infinite permeable vertical plate namely velocity(u), temperature (θ) and concentration (C) profiles as well as the skin friction(τ) have been solved. Graphs of the unsteady velocity, temperature and concentration profiles are presented as well as the skin friction profile in Figs. 1 – 16, to show the influence of the variable parameters on the velocity, temperature, concentration and the skin friction.

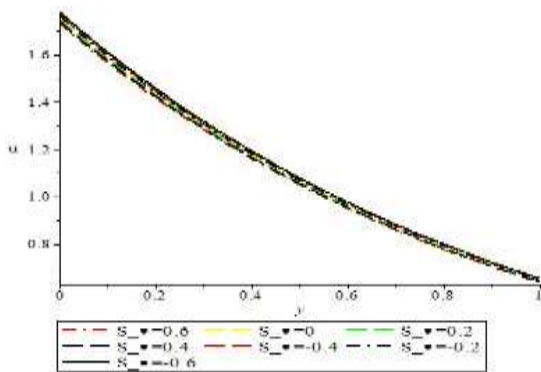


Fig. 1: Effect of S_* on the velocity profile when $t = 0.1, Kr_* = 0.1, Sc = 0.1, Nc = 0.01, Pr = 0.7, R = 1, Ec = 1.5, \alpha_c = 1, Gr = 2, Gm = 3$

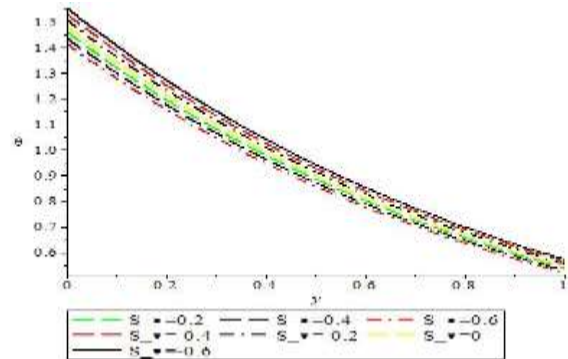


Fig. 2: Effect of S_* on the temperature profile when $t = 0.1, Kr_* = 0.1, Sc = 0.1, Nc = 0.01, Pr = 0.7, R = 1, Ec = 1.5, \alpha_c = 1$

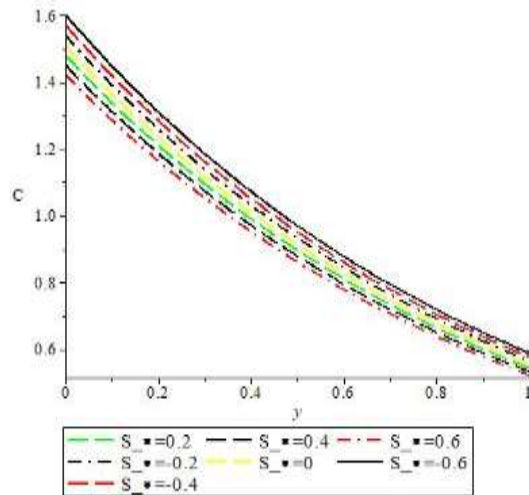


Fig. 3: Effect of S_* on the concentration profile when $t = 0.1, Kr_* = 0.5, Sc = 0.22, Nc = 0.01$

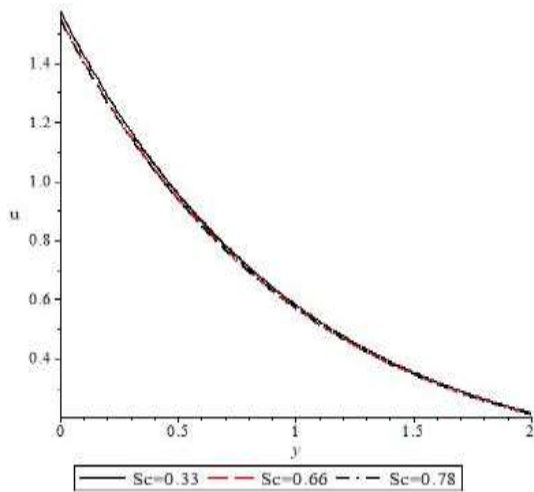


Fig. 4: Effect of Sc on the velocity profile when $t = 0.1, Kr_* = 0.1, S_* = 0.5, Nc = 0.01, Pr = 0.7, R = 1, Ec = 1.5, \alpha_c = 1, Gr = 2, Gm = 3$

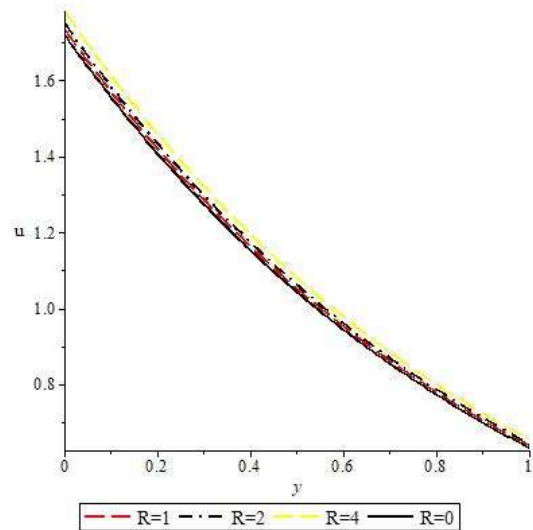


Fig. 7: Effect of R on the velocity profile when $t = 0.1, Kr_* = 0.1, S_* = 0.5, Nc = 0.01, Pr = 0.7, Sc = 0.1, Ec = 1.5, \alpha_c = 1, Gr = 2, Gm = 3$

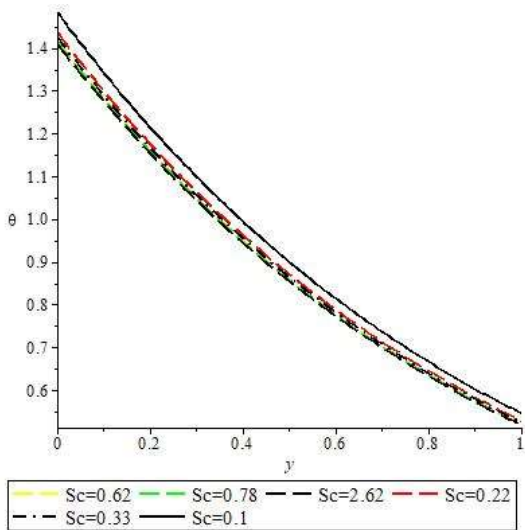


Fig. 5: Effect of Sc on the temperature profile when $t = 0.1, Kr_* = 0.1, S_* = 0, Nc = 0.01, Pr = 0.7, R = 1, Ec = 1.5, \alpha_c = 1$

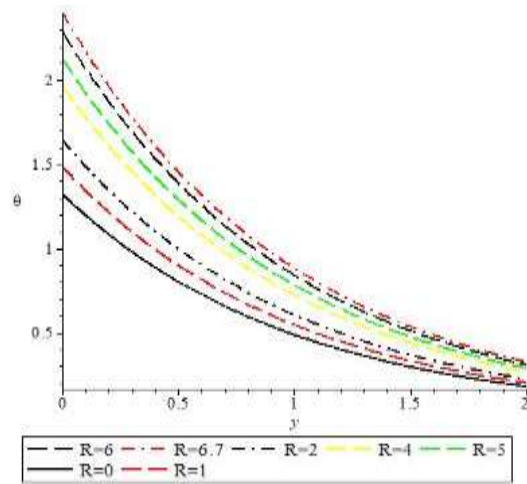


Fig. 8: Effect of R on the temperature profile when $t = 0.1, Kr_* = 0.1, S_* = 0, Nc = 0.01, Pr = 0.7, Sc = 0.1, Ec = 1.5, \alpha_c = 1$

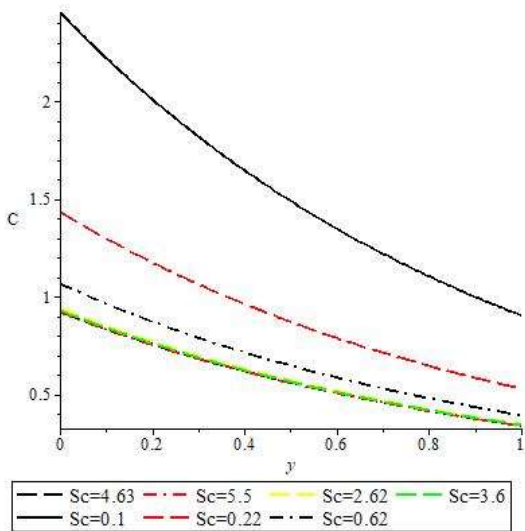


Fig. 6: Effect of Sc on concentration profile when $t = 0.1, Kr_* = 0.5, S_* = 0.5, Nc = 0.01$

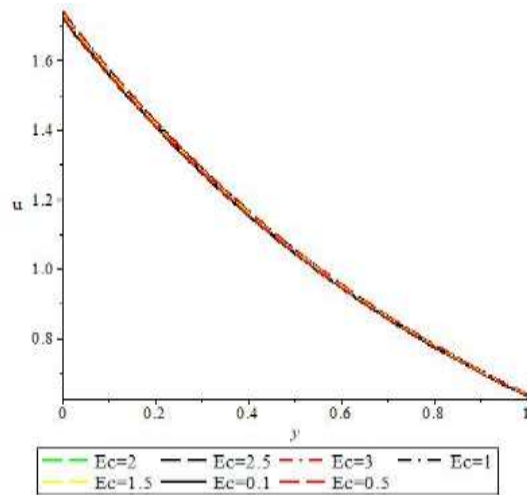


Fig. 9: Effect of Ec on the velocity profile when $t = 0.1, Kr_* = 0.1, S_* = 0.5, Nc = 0.01, Pr = 0.7, Sc = 0.1, R = 0.7, \alpha_c = 1, Gr = 2, Gm = 3$

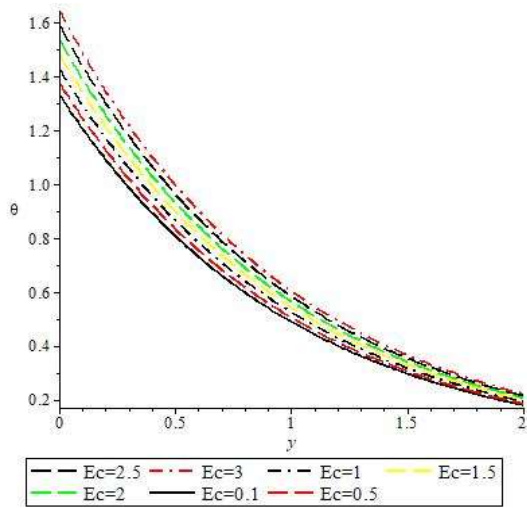


Fig. 10: Effect of Ec on the temperature profile when $t = 0.1, Kr_* = 0.1, S_* = 0, Nc = 0.01, Pr = 0.7, Sc = 0.1, R = 1, \alpha_c = 1$

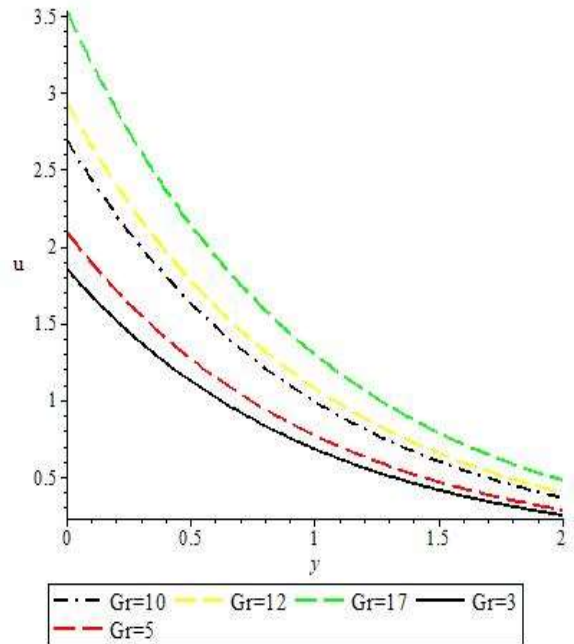


Fig. 13: Effect of Gr on the velocity profile when $t = 0.1, Kr_* = 0.1, S_* = 0.5, Nc = 0.01, Ec = 1.5, Sc = 0.1, R = 1, \alpha_c = 1, Pr = 0.7, Gm = 3$

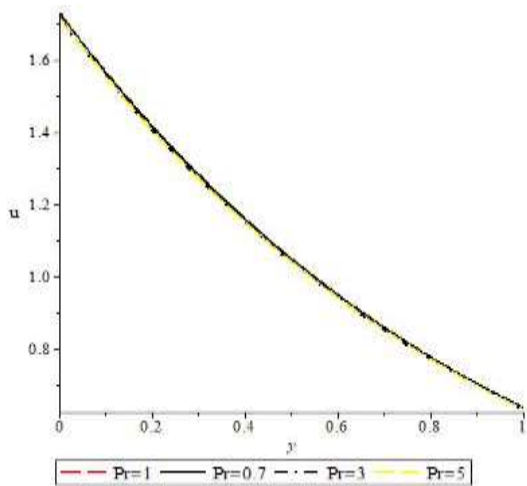


Fig. 11: Effect of Pr on the velocity profile when $t = 0.1, Kr_* = 0.1, S_* = 0.5, Nc = 0.01, Ec = 1.5, Sc = 0.1, R = 0.7, \alpha_c = 1, Gr = 2, Gm = 3$

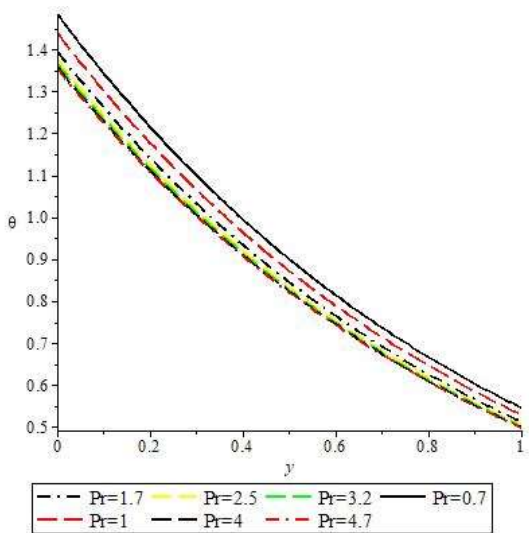


Fig. 12: Effect of Pr on the temperature profile when $t = 0.1, Kr_* = 0.1, S_* = 0, Nc = 0.01, Ec = 1.5, Sc = 0.1, R = 1, \alpha_c = 1$

Figures 1-3 show the variations in velocity, temperature and concentration for different values of suction/injection(S_*). In Fig. 1, velocity of the fluid is observed to decrease as the suction/injection(S_*)parameter increases and a sharp decay is noticed in velocity throughout the plate. In Fig. 2, it is seen that the temperature of the fluid near the plate boundary decreases also as the suction/injection(S_*) parameter increase. Moreover, in Fig. 3, also the concentration of the fluid is seen to decrease as the suction/injection(S_*) parameter increases where a sharp decay is noticed near the plate and further away.

Figures 4 – 6 show the variations in velocity, temperature and concentration for different values of the Schmidt number(Sc). Figure 4 shows that as the Schmidt number increases the velocity of the fluid decreases throughout the medium and converges at a point far from the plate. In Fig. 5, temperature of the fluid is observed to fall at the boundary of the plate as the Schmidt number increases, showing also that as the fluid flows further away from the plate the temperature reduces further. Figure 6 depicts that as the Schmidt number increases, the concentration profile decreases thereby causing the concentration buoyancy effect to decrease which intend bring about a reduction in the fluid concentration.

Figures 7 and 8 show variations in velocity and temperature profiles for different values of the Radiation parameter(R). In Fig. 7, it is seen that as the radiation parameter increases the velocity of the fluid is also seen to increase near the plate boundary and as the fluid further moves away from the plate the velocity tend to reduce over the given distance. Fig. 8 presents that the temperature of the fluid increases at the plate boundary and then reduces rapidly as it tends to move away from the plate as the radiation parameter increases.

Figures 9 and 10 present the variations in velocity and temperature profiles for different values of Eckert number(Ec). Fig. 9 shows an increase in the velocity of the fluid as the Eckert number increases an indication that the fluid flow faster away from the plate boundary. Figure 10 indicates that the temperature of the fluid increases whenever the Eckert number increased.

From Figs. 11 and 12, it is evident from these figures that as the Prandtl number (Pr) increases the velocity is seen to reduce from the boundary of the plate further away. Fig. 12 depicts that the temperature decreases with increase in Prandtl number.

Figure 13 presents the effect of Grashof number (Gr) on the velocity profile and it shows that the velocity increases at the plate boundary as the Grashof number increases. An indication of the momentum boundary thickness generally decreases with increasing Gr since convective boundary layer flow is often associated by injecting or suction of fluid through a permeable surface. In Fig. 14, it is seen that the Radiation absorption parameter (α_c) has an advance effect on the temperature profile. The temperature of the fluid is seen to increase at the boundary of the plate as the radiation absorption parameter increases and also tends to reduce as the fluid moves away from the plate.

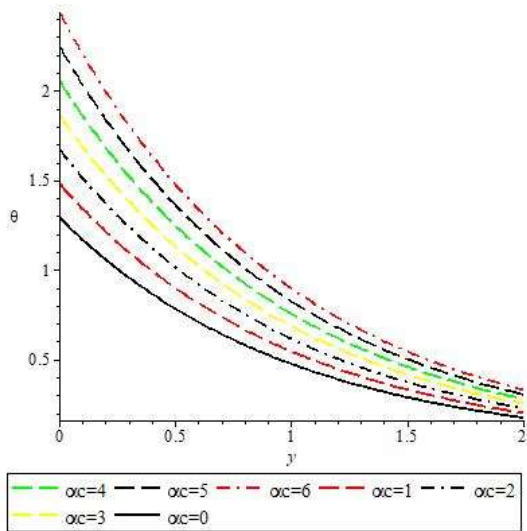


Fig. 14: Effect of α_c on the temperature profile when $t = 0.1, Kr_* = 0.1, S_* = 0, Nc = 0.01, Ec = 1.5, Sc = 0.1, R = 1, Pr = 0.7$

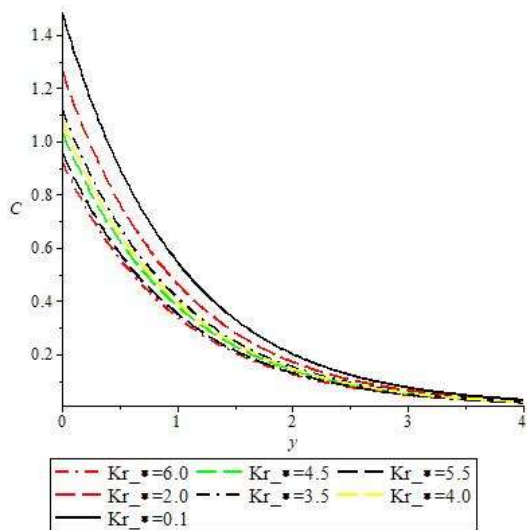


Fig. 15: Effect of Kr_* on concentration profile when $t = 0.1, Sc = 0.22, S_* = 0.5, Nc = 0.01$

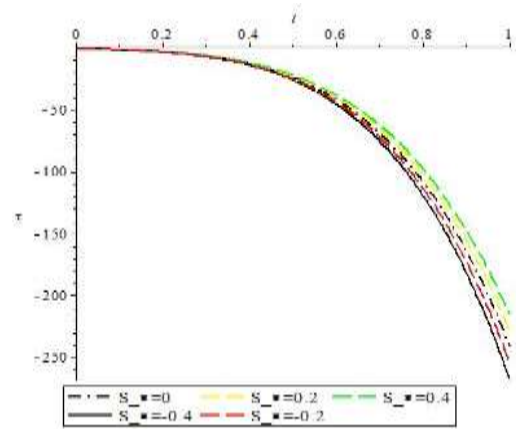


Fig. 16: Effect of S_* on skin-friction profile when $Sc = 0.1, Kr_* = 0.1, \alpha_c = 1, Pr = 0.7, Gm = 3, Gr = 2, R = 1, Ec = 1.5$

Furthermore, Fig. 15 depicts that as the chemical reaction parameter (Kr_*) increases the concentration decreases at the boundary of the plate and also far away from the plate, this is as a result that destructive chemical reduces the solutal boundary layer thickness. Finally, Fig. 16 shows the Skin friction (τ) profile, where the skin friction reduces as suction/injection increases, showing a sharp decay at points close to the plate.

Conclusion

Thermal radiation and chemical reaction effects on an unsteady forced and free convection flow past and infinite permeable vertical plate is presented, where the velocity (u), temperature (θ), concentration (C) and the skin friction (τ) profiles were obtained and solved using the He-Laplace technique. The introduction of thermal radiation and chemical reaction has changed the nature of the flow by Daniel *et al.* (2013).

In the course of this investigation, it is observed that increase in the value of S_* leads to sharp fall in the velocity at the boundary layer, temperature and the concentration of the fluid flow. The velocity of the fluid decreases as the Sc increases and the reverse is the case as the values of R, Ec and Gr increases. Similarly, concentration becomes lower with increase in both Sc and Kr_* . Skin friction (τ) is seen to reduce as suction/injection (S_*) increases at different time intervals.

Conflict of Interest

Authors have declared that there is no conflict of interest reported in this work.

References

Ahmed N, Kahta H & Barua DP 2010. Unsteady MHD free convective flow past a vertical porous plate immersed in a porous medium with hall current, thermal diffusion and heat source. *Int. J. Engr., Sci. and Techn.*, 2(6): 59-74.
 Arifuzzaman SM, Khan MS, Mahedi MFU, Rana BMJ & Ahmmed SF 2018. Chemically reactive and naturally convective high speed MHD fluid flow through an oscillatory vertical plate with heat and radiation absorption effect. *Engr. Sci. and Techn.*, 21: 215-228.
 Babu VS & Reddy KJR 2017. Radiation and chemical reaction effects on unsteady MHD free convection flow past a linearly accelerated vertical porous plate with variable temperature and mass diffusion. *Global J. Pure and Appl. Math.*, 13(9): 5341-5358.

The Effects of Thermal and Chemical Reaction on Unsteady Convection Flow

- Daniel S, Tella Y & Sani U 2013. An unsteady forced and free convection flow past an infinite permeable vertical plate. *Int. J. Sci. and Techn.*, 3(3): 177-183.
- Hradyesh KM & Atulya KN 2012. He-Laplace method for linear and nonlinear partial differential equations. *J. Appl. Math.*, 2012, 1-16.
- Idowu AS & Jimoh A 2017. Effect of thermal conductivity on magneto hydrodynamic heat and mass transfer in porous medium saturated with Kuvshinshiki Fluid. *FUOYE J. Engr. and Techn.*, 2(2): 66-72.
- Javaherdeh K, Nejad MM & Moslemi M 2015. Natural convection heat and mass transfer in MHD fluid flow past a moving vertical plate with variable surface temperature and concentration in a porous medium. *Engr. Sci. and Techn.*, 18: 423-431.
- Malapati V & Polarapu P 2015. Unsteady MHD free convective heat and mass transfer in a boundary layer flow past a vertical permeable plate with thermal radiation and chemical reaction. *Procedia Engineering*, 127: 791-799.
- Narahari M & Nayan MY 2011. Free convection flow past an impulsively started infinite vertical plate with newtonian heating in the presence of thermal radiation and mass diffusion. *Turkish J. Engr. and Envtal. Sci.*, 35: 187-198.
- Rao BM, Reddy GV, Raju MC & Verma SVK 2013. Unsteady MHD free convective heat and mass transfer flow past a semi-infinite vertical permeable moving plate with heat absorption, radiation, chemical reaction and Soret effects. *Int. J. Engr. Sci. and Emerging Techn.*, 6(2): 241-257.
- Sharma PK 2005. Fluctuating thermal and mass diffusion on unsteady free convection flow past a vertical plate in slip-flow regime. *Latin Am. Appl. Res.*, 35: 313-319.
- Shivaiah S & Rao JA 2012. Chemical reaction effect on an unsteady MHD free convection flow past a vertical porous plate in the presence of suction or injection. *Theoretical Applied Mechanics*, 39(2): 185-208.
- Srilatha P & Shekar MNR 2018. Effects of thermal radiation and MHD on the unsteady free convection and mass transform flow past an exponentially accelerated vertical plate with variable temperature a finite element solution. *Int. J. Mechan. Engr. and Techn.*, 9(5): 358-370.
- Vedavathi N, Ramakrishna K & Reddy KJ 2014. Radiation and mass transfer effects on unsteady MHD convective flow past an infinite vertical plate with Daffour and Soret effects. *Ain. Shams Engr. J.*, 6: 363-371.